

Structure and Electron Delocalization in Al_4^{2-} and Al_4^{4-}

Rafael Islas,^{†,§} Thomas Heine,^{*,§} and Gabriel Merino^{*,‡}

Facultad de Química, Universidad de Guanajuato, Noria Alta s/n, Guanajuato, Gto, 36050, México, and Institut für Physikalische Chemie und Elektrochemie, TU Dresden, D-01062 Dresden, Germany

Received January 10, 2007

Abstract: Structure, dynamics, and electron delocalization of Al_4^{2-} and Al_4^{4-} based clusters are investigated. Gradient-corrected Density-Functional Born–Oppenheimer Molecular Dynamics simulations indicate that Al_4^{2-} based clusters have a rigid planar Al framework, while the Al_4^{4-} based moieties show large distortions from planarity. The induced magnetic field analysis of these species indicates that both systems have diatropic σ -systems, while the π -system is diatropic for Al_4^{2-} and paratropic for Al_4^{4-} . The total magnetic response is diatropic for Al_4^{2-} , while Al_4^{4-} is “bitropic”: it has typical antiaromatic long-range cones, while the magnetic field in the Al_4^{4-} ring plane is similar to that of aromatic annulenes.

1. Introduction

Aromaticity is the simplest way to explain the stability of unsaturated cyclic hydrocarbons with $(4n + 2)$ electrons delocalized in π -orbitals perpendicular to the ring plane.¹ Even though the introduction of the aromaticity concept in chemistry is quite old, its definition is still controversial. In view of these problems of subjectivity, it is remarkable that aromaticity is useful to rationalize and understand the structure and reactivity of many organic molecules. In 1971, Wade proposed a similar concept to describe delocalized σ -bonding in closed-shell boron deltahedra, which follow a $2n+2$ skeletal electron rule.^{2,3} This concept has been extended by Hirsch to treat spherical clusters by his $2(n+1)^2$ rule,⁴ and various applications to organic and inorganic clusters have been reported.^{5,6} However, stability based on aromaticity had not been confirmed for any metallic moiety until Li et al. published their seminal paper entitled “*Observation of all-metal aromatic molecules*”.⁷

A series of compounds consisting of a square planar Al_4^{2-} , face-capped by an M^+ cation ($\text{M}=\text{Li}, \text{Na}, \text{Cu}$), were produced by laser vaporization, and their electronic spectra were obtained using negative ion photoelectron spectroscopy.

Li et al. found that theoretical vertical detachment energies of the pyramidal structures are in excellent agreement with the experimental spectra, thereby suggesting that C_{4v} structures are the global minima for the MAl_4^- species.

Ab initio calculations show that Al_4^{2-} have two electrons residing in a π -orbital, satisfying the Hückel rule for aromatic compounds. Li et al.⁷ concluded that this π -orbital holds “*the key to understanding the structure and bonding of MAl_4^- species*”. However, electron delocalization in Al_4^{2-} is not so simple. There are two delocalized σ -bonding orbitals (HOMO-1 and HOMO-2) spread across all four aluminum atoms. Therefore, the stability of Al_4^{2-} has been ascribed to its doubly aromatic behavior (π - and σ -aromaticity), which is different from hydrocarbon aromatic molecules.^{7,8} Similar systems inhibiting double aromaticity, Ga_4^{2-} and In_4^{2-} ,⁹ and in valence-isoelectronic Hg_4^{6-} ,¹⁰ have been discussed earlier. Aromaticity and electron delocalization of Al_4^{2-} have been studied in detail.^{11,12} Fowler et al. evaluated the ring current in Al_4^{2-} and MAl_4^- ($\text{M}=\text{Li}, \text{Na}, \text{Cu}$) and concluded that σ -electrons are responsible for the delocalized diatropic current induced by a perpendicular magnetic field.^{13,14} A diatropic (diamagnetic) current results in a shielded applied magnetic field, while a paratropic (paramagnetic) current has opposite direction and deshielding. Based on the analysis of aromatic ring-current shielding calculations (ARCS),¹⁵ Juse-lius et al. concluded that π -electrons contribute to the diatropic ring current, and thus Al_4^{2-} is both σ - and π -aromatic,¹⁶ while a recent analysis of Havenith and Fowler

[†] Dedicated to Professor Dennis R. Salahub on the occasion of his 60th birthday.

^{*} Corresponding author e-mail: gmerino@quijote.ugto.mx (G.M.) and thomas.heine@chemie.tu-dresden.de (T.H.).

[‡] Universidad de Guanajuato.

[§] TU Dresden.

showed that the contributions of the π -system to the ring current is significantly smaller than that of the σ -system.¹⁷ This is opposite to the magnetic character of annulenes, which is essentially determined by the π -subsystem. Santos et al. have studied both the total and the σ - π separated electron localization function (ELF)^{18,19} of several molecules.²⁰ They found that Al_4^{2-} has a surprisingly high ELF_π bifurcation value of 0.99, which is even higher than the value associated with benzene. At the same time, Al_4^{2-} shows a high bifurcation value of ELF_σ (0.88), which suggests strong σ -delocalization. Further evidence of the σ -delocalization in Al_4^{2-} can be given by the analysis of the individual canonical molecular orbital contributions to NICS (MO-NICS). Within gradient-corrected DFT, the six σ -orbitals contribute more than 50% of the diatropicity of Al_4^{2-} , while the sum of the MO-NICS contributions^{21,22} of the σ -orbitals in both benzene and D_{2h} cyclobutadiene is positive (paratropic).²³ Al_4^{2-} has also been studied employing the gauge-independent magnetic induced currents (GIMIC).²⁴ With GIMIC, integrated current densities can easily be produced, which supplement information from current density maps with integrated information. In addition, it is possible to subtract disturbing effects coming from surrounding Li cations. The GIMIC method clearly shows that the Al_4^{2-} moiety is diatropic, and no paratropic current is observed.

Boldyrev and Kuznetsov obtained a rough evaluation of the resonance energies for Na_2Al_4 .²⁵ The resonance energies are high: 125 kJ mol⁻¹ (B3LYP/6-311+G*) and 200 kJ mol⁻¹ (CCSD(T)/6-311+G(2df)) compared to 83 kJ mol⁻¹ in benzene. However, it should be noted that it is hard to accurately evaluate the resonance energy in this cluster due to two factors: the interaction between Na^+ and Al_4^{2-} and the problem of identifying a reference molecule with an Al–Al double bond. Zhan et al. concluded that in terms of the magnitude of the Dewar resonance energy,⁸ the aromaticity of the Al_4^{2-} is multiple-fold as compared to the usual “1-fold” aromaticity of benzene.⁸ Al_4^{2-} can be represented by 64 potentially resonating Kekulé-like structures; each Kekulé-like structure has three localized chemical bonds, compared to only two Kekulé structures of benzene. Consequently, the resonance energy of Al_4^{2-} (~ 304 kJ mol⁻¹ as the upper limit and ~ 220 kJ mol⁻¹ as the lower limit) is at least 2.5 times that of benzene. Therefore, Al_4^{2-} could be considered as a “3-fold” aromatic system.

In 2003, Kuznetsov et al. proposed that the Al_4^{4-} fragment would be a good candidate to be the first antiaromatic all-metal system: if two additional electrons enter the π -system, Al_4^{4-} will be antiaromatic within Hückel theory.²⁶ They stated that the deviation from an equilateral square ring confirms that the compound is antiaromatic. In the same year, Chen et al. argued that the Al_4Li_3^- species is *aromatic* rather than antiaromatic, due to the predominating effects of σ -aromaticity over π -antiaromaticity.²³ Havenith et al. pointed out the mixed character of Al_4Li_3^- and Al_4Li_4 : It shows a diatropic current in the molecular plane, but a paratropic one out-of-plane.²⁷ This lively discussion has been reviewed by Boldyrev et al.¹² and Tshipis et al.²⁸

In this work, we study Al_4^{2-} and Al_4^{4-} cores in two ways: First, we perform molecular dynamics simulations to

understand the role of the Li counterions. Are they only suppliers of charge, or do they play a more important role for these clusters? Then, cognizant of the difficulties in assigning an aromatic or antiaromatic character to these clusters, we nevertheless try to improve our understanding of electron delocalization of Al_4^{2-} and Al_4^{4-} using the induced magnetic field (\mathbf{B}^{ind}).²⁹ We calculate the contributions of the π - and of the σ -electrons to the magnetic field individually.³⁰ With the full magnetic response of the cluster it is easier to distinguish local effects of the Li ions from those of the Al_4^{n-} clusters, and a more detailed interpretation of the results is possible.

II. Computational Details

Structures were optimized using Becke's exchange (B),³¹ Lee, Yang and Parr (LYP) correlation,³² and within the hybrid functional (B3LYP) approach, as implemented in Gaussian. All geometrical optimizations were done using the 6-311++G(2df) basis set.^{33,34} The NMR calculations were performed using the PW91 functional and IGLO-III basis set.³⁵ Cartesian shielding tensors were computed using the IGLO method.³⁶ The deMon program³⁷ was used to compute the molecular orbitals and the deMon-NMR package^{38,39} for the shielding tensors. Induced magnetic fields²⁹ were computed by

$$\mathbf{B}^{\text{ind}}(\mathbf{R}) = -\sigma_{\alpha\beta}(\mathbf{R})\mathbf{B}^{\text{ext}} \quad (1)$$

from Cartesian shielding tensors and are in ppm of the units of the external field. Assuming an external magnetic field of $|\mathbf{B}^{\text{ext}}| = 1.0$ T, the unit of the induced field is 1.0 μT , which is equivalent to 1.0 ppm of the shielding tensor. VU⁴⁰ was employed for visualization of the induced field vectors, their contour lines, and isosurfaces. The σ - and π -contributions to the induced magnetic field have been separated using the IGLO method, where localized molecular orbitals (LMOs) have been created using the procedure suggested by Pipek and Mezey.⁴¹ We have chosen a LMO representation⁴² in favor over a canonical MO representation,^{21,22,43} as this approach has been proven to give reliable results for annulenes³⁰ and is computationally advantageous.

Born–Oppenheimer Molecular dynamics simulations have been performed at the PBE³³/DZVP³⁴ level within the NVT (constant number of particles, volume, and temperature) ensemble⁴⁴ using deMon.³⁷ After equilibration, trajectories of up to 25 ps were produced at temperatures of 300 K and 600 K, with a temperature coupling constant $\tau = 0.5$ ps and a time step of 0.5 fs.⁴⁴

III. Results and Discussion

It is not straightforward to separate the magnetic response of planar Al_4^{2-} and Al_4^{4-} clusters into σ - and π -contributions. While for hydrocarbons it is clear that the stabilization of planar rings is due to the π -electrons and Hückel theory is applicable in a simple way, it is well-known that for metal clusters the situation is not so simple: Both, σ - and π -systems, show a large degree of delocalization, which is a result of the small number of electrons in both electronic subsystems and the ring topology, which favors delocalized

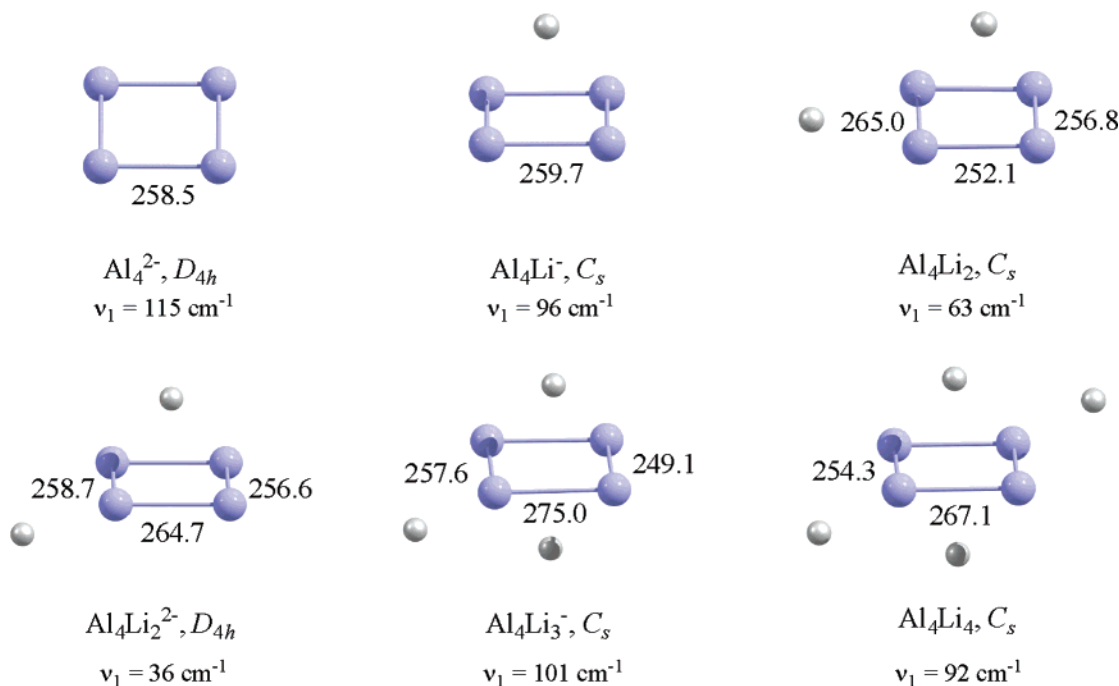


Figure 1. Optimized geometries of the title systems calculated with B3LYP/6-311++G(2df). Bond lengths are given in picometers.

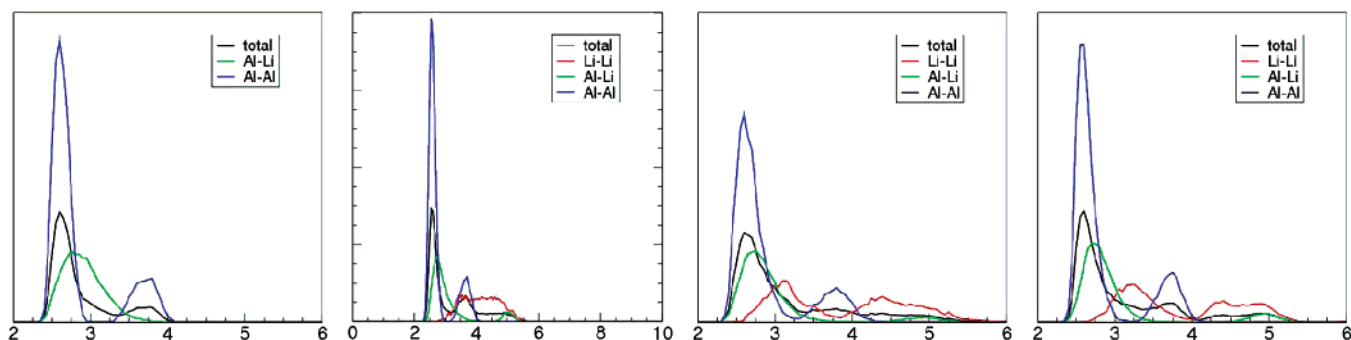


Figure 2. Pair distribution functions, taken from MD trajectories at 300 K of (from left to right) Al_4Li^- , Al_4Li_2 , Al_4Li_3^- , and Al_4Li_4 . Distances are given in Å, and all functions follow identical normalization criteria.

electrons.^{12–14,16,17,26–28,43,45–48} Further, the calculation of highly anionic species often results in technical problems as convergence failures. Therefore, we studied closed-shell clusters with an increasing number of Li^+ counterions, starting from Al_4^{2-} , Al_4Li^- , Al_4Li_2 , Al_4Li_3^- , and Al_4Li_4 .

A. Structure. As can be seen from Figure 1, the geometries depend only slightly on the number of counter charges as long as the formal charge of the Al_4 backbone is maintained. While the bond lengths differ by 7 pm in the dianion (keeping the quadratic form of the metal frame), the bond lengths differs by 35 pm in Al_4Li_3^- , i.e., the ground state of Li_3Al_4^- possesses a distorted rectangular Al_4 framework. Shaik et al. stated that even if there is a distortion from the square structure in Li_3Al_4^- , it is an aromatic system because of the distortive nature of π -electrons.⁴⁹ Juselius et al. used the ARCS method to show that Al_4^{4-} is antiaromatic and concluded that the normally reliable NICS calculations failed in this case.¹⁶ It is a lively discussion. But there still remains a simple question: are the lithium atoms only suppliers of charge, or do they play a more important role for these clusters.

Our molecular dynamics simulations show that the stability of the positions of the lithium atoms depends strongly on the cluster. For Al_4Li^- , the lithium atom sits on top of the ring and does not leave this position during a trajectory of 25 ps at 300 K. It shows, however, large amplitude movements parallel to the ring, partially hopping to the corners and back to the position on top of the ring center. The lowest vibrational frequency of this cluster, 96 cm^{-1} , corresponds to this movement of the lithium atom. The pair distribution function (PDF) (Figure 2) indicates the large fluxionality of the Li ion by the very broad Al–Li signal. The sharp Al–Al signal indicates that within the resolution of the PDF the bond lengths are equalized.

Opposite to simple electrostatic expectations, the second Li cation in Al_4Li_2 is not located at the opposite ring site, forming a bipyramidal cluster, it rather sits on top of an Al–Al bond. The structure of Al_4Li_2 is more fluxional than that of Al_4Li^- , as the electrostatic attraction between ring and cations is weaker and also as both cations repel each other and show collective motions. In particular the Li atom sitting on the bond shows large amplitude motions. This is

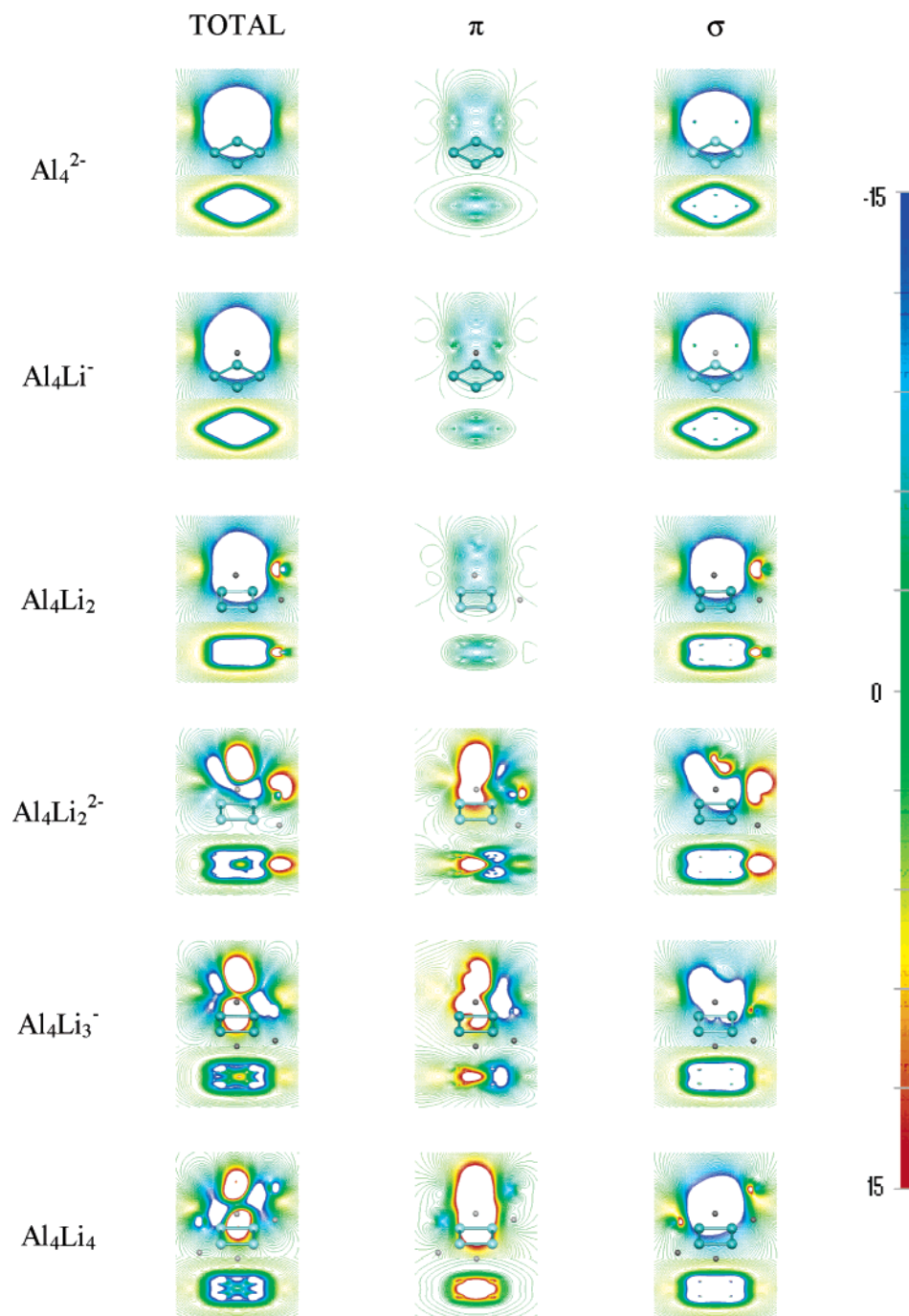


Figure 3. Contour lines of the z-component of \mathbf{B}^{ind} in the molecular plane and perpendicular to the molecular plane through the origin. The scale is given in ppm or μT for an external field of 1 T.

also visible in the PDF, where the Li–Li signal is very broad, similar to that of a liquid.

For Al_4Li_3^- we observe the largest fluxionality. The influence on the Al–Al bond length by the neighboring cations is visible by the much wider Al–Al signal, even though the resolution of the PDF cannot distinguish between different Al–Al bond lengths. During a 25 ps simulation, even at 300 K, Li atoms hop between different sites, which is reflected by the widely spread Li–Li signal. For Al_4Li_4 , the Al–Al distances show a similar distribution as for Al_4Li^- , while the fluxionality of the Li atoms is similar as in Al_4Li_3^- . Also here, Li atoms exchange positions during the simulation.

B. Electron Delocalization. The degree of aromaticity of the Al_4^{2-} and Al_4^{4-} anions has been studied using different theoretical schemes. They include the plotting of ring current densities,^{13,17,47} further quantified by the calculation of GIMIC ring currents above and below the ring,⁴⁶ and an analysis on MO-resolved nucleus-independent chemical shifts.⁴⁸ For Al_4^{2-} , a σ - and π -resolved NICS analysis is available.²³ These results have been summarized in a special issue of *Chemical Reviews* devoted to electron delocalization.^{11,12}

It is agreed that the σ -system contributes strongly to the aromatic character of both Al_4^{2-} and Al_4^{4-} frameworks. There is also no argument that the π -contribution of Al_4^{2-} is diatropic, as there is only a single occupied π -orbital, and

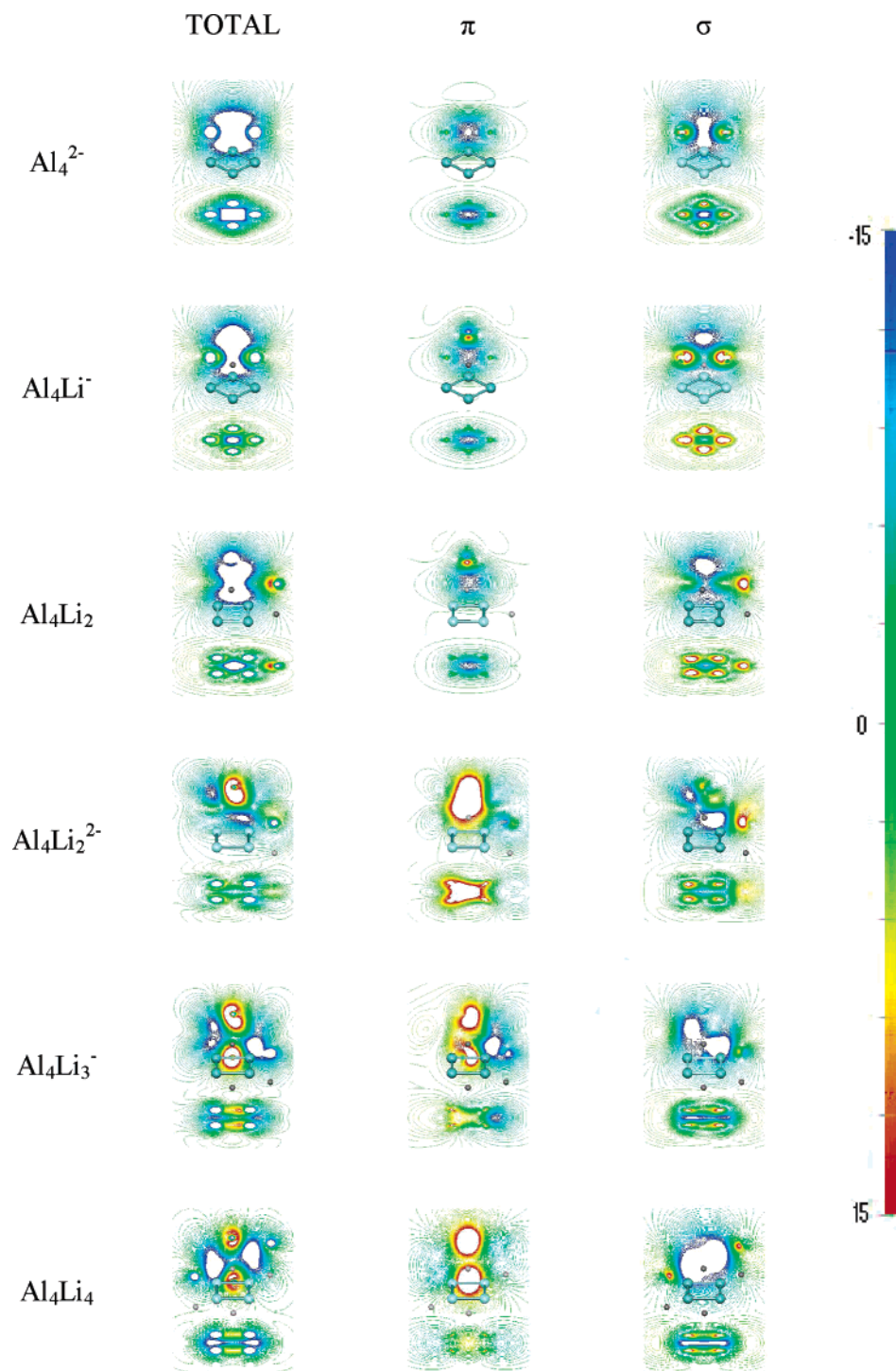


Figure 4. Contour lines of NICS parameter in the molecular plane and perpendicular to the molecular plane through the origin. The scale is given in ppm or μT for an external field of 1 T.

that the π -contribution in Al_4^{4-} species is paratropic. There is, however, disagreement as to whether Al_4^{4-} should be called an aromatic or an antiaromatic molecule.²³ The argument of Boldyrev and Wang states that there is a paratropic π -system which is occupied as in classical antiaromatic hydrocarbons, i.e., C_4H_4 . Furthermore, the π -states of Al_4^{4-} are degenerate, leading to a Jahn–Teller-like distortion similar to for C_4H_4 . The response of Chen and others is that the antiaromatic effect of the π -system is overwhelmed by the aromatic effect of the σ -system.

In agreement, the ring current maps of Havenith et al. show that the current through the π -orbitals is not significant.^{17,27}

We plotted the σ - and π -separated z -components of the induced magnetic fields, which coincide with the NICS_{zz} index at the ring center⁴⁹ (Figure 3), and of $\text{NICS}(\mathbf{r})$ (Figure 4).

In Figure 3, the z -component of the induced magnetic field, applied perpendicular to the ring, is shown for Al_2^{2-} and Al_4^{4-} based species. For the Al_2^{2-} moieties, the total magnetic

response is quite similar to that of aromatic hydrocarbons.³⁰ For Al_4^{4-} , the situation is not that clear. The shielding cones of the molecule on top and bottom, induced by the π -electrons, is comparable to that of cyclobutadiene,³⁰ though smaller in magnitude and perturbed by the Li ions. Closer to the ring plane and at positions far from the ring center, however, the response is aromatic and similar to that of an aromatic hydrocarbon. The same magnetic response applied to C_4H_4 would result in aromatic protons. It is therefore difficult to make a final statement as to whether Al_4^{4-} should be called aromatic or antiaromatic. Evidently, NICS can fail near the ring center. Therefore, the NICS or z -component of \mathbf{B}^{ind} isolines or isosurfaces give us important (but still partial) insight into electron delocalization.

It is, however, clear that σ - and π -components of Al_4^{4-} show an opposite response. The σ -system is evidently diatropic and very similar to that of Al_4^{2-} . On the other hand, the π -systems of Al_4^{4-} moieties show a typical antiaromatic response, as in an antiaromatic annulene, e.g., C_4H_4 . In agreement with previous studies,^{17,23,27} for Al_4^{2-} , the contribution of the π -system is small compared to the σ -system.

The advantage of a complete response map over a single magnetic index is obvious: For the Al_4^{4-} species, the z -component of the \mathbf{B}^{ind} index will deliver a small number, indicating either a small net para- or diatropicity. The NICS-(1) family of indices, and even the ARCS approach,¹⁵ will sense the paratropic π -system, as no information of the outer ring areas enter. The complete map of the induced magnetic field, however, shows the “bitropic” character of the molecule: there is a diatropic contribution raised by the σ -electrons which dominates in the ring plane and a paratropic part, induced by the π -system around the z -axis. The same effect is visible in ring current maps at different height profile.²⁷ In contrast to many other molecules as hydrocarbons,³⁰ both contributions are significant.

IV. Conclusions

Our calculations show that Al_4^{2-} and Al_4^{4-} based metal clusters cannot be discussed isolated from the counterions: They not only stabilize the Al_4^{n-} anions electrostatically but also have an influence on the chemical structure. Molecular dynamics simulations show that the cations are relatively fixed for Al_4Li^+ and Al_4Li_2 but become more floppy for Al_4Li_3^+ and Al_4Li_4 . For these molecules, any static structural representation is not realistic.

Magnetically, the induced magnetic field representation agrees with former investigations based on NICS and ring current calculations concerning the character of the σ - and π -systems. For the total response, our computations show that a simple classification of a molecule as “aromatic” or “antiaromatic” is impossible for those systems containing a Al_4^{4-} backbone, at least as long as this term does not have a more strict definition. For this case, the complete map of the induced magnetic field shows the “bitropic” character of the molecule, the diatropic contribution raised by the σ -electrons which dominates in the ring plane, and the paratropic part, induced by the π -system around the z -axis. While the long-range response perpendicular to the molecular planes is typical, though smaller in magnitude, for molecules

with aromatic (Al_4^{2-}) and antiaromatic (Al_4^{4-}) π -systems, respectively, the response in the ring planes is similar to that of aromatic molecules.

Acknowledgment. This work was funded in part by grants from PROMEP-SEP (project UGTO-PTC-079), DIN-PO-UGTO, and the Deutsche Forschungsgemeinschaft (DFG).

Supporting Information Available: Coordinates of the optimized structures, vibrational frequencies, and energies. This material is available free of charge via the Internet at <http://pubs.acs.org>.

References

- (1) Schleyer, P. v. R. *Chem. Rev.* **2001**, *101*, 1115.
- (2) Wade, K. *Chem. Commun.* **1971**, 792.
- (3) Srinivas, G. N.; Anoop, A.; Jemmis, E. D.; Hamilton, T. P.; Lammertsma, K.; Leszczynski, J.; Schaefer, H. F. *J. Am. Chem. Soc.* **2003**, *125*, 16397.
- (4) Hirsch, A.; Chen, Z. F.; Jiao, H. J. *Angew. Chem., Int. Ed.* **2001**, *40*, 2834.
- (5) King, R. B.; Heine, T.; Corminboeuf, C.; Schleyer, P. v. R. *J. Am. Chem. Soc.* **2004**, *126*, 430.
- (6) Chen, Z. F.; King, R. B. *Chem. Rev.* **2005**, *105*, 3613.
- (7) Li, X.; Kuznetsov, A. E.; Zhang, H. F.; Boldyrev, A. I.; Wang, L. S. *Science* **2001**, *291*, 859.
- (8) Zhan, C. G.; Zheng, F.; Dixon, D. A. *J. Am. Chem. Soc.* **2002**, *124*, 14795.
- (9) Kuznetsov, A. E.; Boldyrev, A. I.; Li, X.; Wang, L. S. *J. Am. Chem. Soc.* **2001**, *123*, 8825.
- (10) Kuznetsov, A. E.; Corbett, J. D.; Wang, L. S.; Boldyrev, A. I. *Angew. Chem., Int. Ed. Engl.* **2001**, *40*, 3369.
- (11) Heine, T.; Corminboeuf, C.; Seifert, G. *Chem. Rev.* **2005**, *105*, 3889.
- (12) Boldyrev, A. I.; Wang, L. S. *Chem. Rev.* **2005**, *105*, 3716.
- (13) Fowler, P. W.; Havenith, R. W. A.; Steiner, E. *Chem. Phys. Lett.* **2001**, *342*, 85.
- (14) Fowler, P. W.; Havenith, R. W. A.; Steiner, E. *Chem. Phys. Lett.* **2002**, *359*, 530.
- (15) Juselius, J.; Sundholm, D. *Phys. Chem. Chem. Phys.* **1999**, *1*, 3429.
- (16) Juselius, J.; Straka, M.; Sundholm, D. *J. Phys. Chem. A* **2001**, *105*, 9939.
- (17) Havenith, R. W. A.; Fowler, P. W. *Phys. Chem. Chem. Phys.* **2006**, *8*, 3383.
- (18) Becke, A. D.; Edgecombe, K. E. *J. Chem. Phys.* **1990**, *92*, 5397.
- (19) Silvi, B.; Savin, A. *Nature* **1994**, *371*, 683.
- (20) Santos, J. C.; Tiznado, W.; Contreras, R.; Fuentealba, P. *J. Chem. Phys.* **2004**, *120*, 1670.
- (21) Corminboeuf, C.; Heine, T.; Weber, J. *Phys. Chem. Chem. Phys.* **2003**, *5*, 246.
- (22) Heine, T.; Schleyer, P. v. R.; Corminboeuf, C.; Seifert, G.; Reviakine, R.; Weber, J. *J. Phys. Chem. A* **2003**, *107*, 6470.
- (23) Chen, Z. F.; Corminboeuf, C.; Heine, T.; Bohmann, J.; Schleyer, P. v. R. *J. Am. Chem. Soc.* **2003**, *125*, 13930.

- (24) Juselius, J.; Sundholm, D.; Gauss, J. *J. Chem. Phys.* **2004**, *121*, 3952.
- (25) Boldyrev, A. I.; Kuznetsov, A. E. *Inorg. Chem.* **2002**, *41*, 532.
- (26) Kuznetsov, A. E.; Birch, K. A.; Boldyrev, A. I.; Li, X.; Zhai, H. J.; Wang, L. S. *Science* **2003**, *300*, 622.
- (27) Havenith, R. W. A.; Fowler, P. W.; Steiner, E.; Shetty, S.; Kanhere, D.; Pal, S. *Phys. Chem. Chem. Phys.* **2004**, *6*, 285.
- (28) Tsepis, C. A. *Coord. Chem. Rev.* **2005**, *249*, 2740.
- (29) Merino, G.; Heine, T.; Seifert, G. *Chem. Eur. J.* **2004**, *10*, 4367.
- (30) Heine, T.; Islas, R.; Merino, G. *J. Comp. Chem.* **2007**, *28*, 302.
- (31) Becke, A. D. *J. Chem. Phys.* **1993**, *98*, 5648.
- (32) Lee, C. T.; Yang, W. T.; Parr, R. G. *Phys. Rev. B* **1988**, *37*, 785.
- (33) Perdew, J. P.; Wang, Y. *Phys. Rev. B* **1992**, *45*, 13244.
- (34) Godbout, N.; Salahub, D. R.; Andzelm, J.; Wimmer, E. *Can. J. Chem.* **1992**, *70*, 560.
- (35) Kutzelnigg, W.; Fleischer, U.; Schindler, M. *The IGLO-Method: Ab Initio Calculation and Interpretation of NMR Chemical Shifts and Magnetic Susceptibilities*; Springer-Verlag: Heidelberg, 1990; Vol. 23.
- (36) Kutzelnigg, W. *Isr. J. Chem.* **1980**, *19*, 193.
- (37) Köster, A. M.; Calaminici, P.; del Campo, J. M.; Casida, M. E.; Flores-Moreno, R.; Geudtner, G.; Goursot, A.; Heine, T.; Ipatov, A.; Janetzko, F.; Patchkovskii, S.; Reveles, J. U.; Salahub, D. R.; Vela, A. *deMon*, 2.2.1; Mexico, Ottawa, Calgary, 2005.
- (38) Malkin, V. G.; Malkina, O. L.; Reviakine, R.; Schimmelpfennig, B.; Arbuznikov, V.; Kaupp, M. *MAG-ReSpect 1.0*, *MAG-ReSpect 1.0*; 2001.
- (39) Malkin, V. G.; Malkina, O. L.; Salahub, D. R. *Chem. Phys. Lett.* **1993**, *204*, 80.
- (40) Ozell, B.; Camarero, R.; Garon, A.; Guibault, F. *Finite Elem. Des.* **1995**, *19*, 295.
- (41) Pipek, J.; Mezey, P. G. *J. Chem. Phys.* **1989**, *90*, 4916.
- (42) Schleyer, P. v. R.; Jiao, H. J.; Hommes, N. J. R. V.; Malkin, V. G.; Malkina, O. L. *J. Am. Chem. Soc.* **1997**, *119*, 12669.
- (43) Corminboeuf, C.; Heine, T.; Seifert, G.; Schleyer, P. v. R.; Weber, J. *Phys. Chem. Chem. Phys.* **2004**, *6*, 273.
- (44) Berendsen, H. J. C.; Postma, J. P. M.; Van Gunsteren, W. F.; Di Nola, A.; Haak, J. R. *J. Chem. Phys.* **1984**, *81*, 3684.
- (45) Lin, Y. C.; Sundholm, D.; Juselius, J.; Cui, L. F.; Li, X.; Zhai, H. J.; Wang, L. S., *J. Phys. Chem. A* **2006**, *110*, 4244.
- (46) Lin, Y. C.; Juselius, J.; Sundholm, D.; Gauss, J. *J. Chem. Phys.* **2005**, *122*.
- (47) Havenith, R. W. A.; Fowler, P. W.; Steiner, E. *Chem. Eur. J.* **2002**, *8*, 1068.
- (48) Fowler, P. W.; Rogowska, A.; Soncini, A.; Lillington, M.; Olson, L. P. *J. Org. Chem.* **2006**, *71*, 6459.
- (49) Jug, K.; Hiberty, P. C.; Shaik, S. *Chem. Rev.* **2001**, *101*, 1477.

CT700009K